Materials Transactions, Vol. 42, No. 9 (2001) pp. 1870 to 1873

Secondary Electron Emission Characteristics of MgO Thin Films Prepared by an Advanced Ion-Plating Method *

Kazuo Uetani[1], Hiroshi Kajiyama[2,3], Akira Kato[2], Akiko Takagi[4], Takanobu Hori[1], Isao Tokomoto[1], Yasuhiro Koizumi[1], Koichi Nose[1], Yasushi Ihara[2], Ken-ichi Onisawa[2] and Tetsuroh Minemura[2]

[1]*R&D Center, ShinMaywa Industries, Ltd., Hyogo 663-8001, Japan*
[2]*Hitachi Research Laboratory, Hitachi, Ltd., Ibaraki 319-1292, Japan*
[3]*Graduate School of Engineering, Ibaraki University, Ibaraki 316-8511, Japan*
[4]*Graduate Student, Ibaraki University, Ibaraki 316-8511, Japan*

We measured the secondary electron emission (SEE) and the film microstructures of the MgO thin films. The films were deposited by the advanced ion-plating (AIP) method we developed and also a conventional electron beam evaporation (EB) method for reference. The secondary electron yield, γ, defined as a ratio of irradiated ion current to emitted electron current of the samples was measured to be 0.55 for the AIP film and 0.35 for the EB film. Scanning electron microscopy (SEM) and atomic force microscopy (AFM) observations revealed that the AIP film had well-defined columnar structures which were grown from the substrate interface to the film surface. The AIP film with thickness of a 100 nm had (111) preferred orientation, while the crystal orientation of the EB film was not detected. We supposed that the γ value was greatly improved due to the improved crystallinity as well as (111) preferred orientation.

(Received April 26, 2001; Accepted June 19, 2001)

Keywords: *plasma display panel, magnesium oxide, protective layer, advanced ion-plating, secondary electron emission*

1. Introduction

Plasma display panel (PDP) is a self-emitting flat panel display using UV radiation generated from rare gas discharge.[1)] PDP has two methods to generate plasma; a direct current (DC) and an alternating current (AC) field type. AC-PDP is being widely commercialized for public and individual use. Figure 1 shows a schematic diagram of a typical AC-PDP. The Ne and Xe gas plasma is induced by the voltage applied between two sustain electrodes and then emits UV lights. These UV lights excite phosphors that emit visible lights of three primary colors in red, green and blue.

The ion bombardment from Ne and Xe plasma seriously damages the dielectric layer and sustain electrodes, shortly leading to the breakdown of stable plasma generation. Thus, a kind of protective layer made of transparent and anti-sputtering materials must be coated on top of front panels. The protective layer has one more important role of reducing discharge voltages by secondary electron emission (SEE) from the protective layer itself induced by ion bombardment. Magnesium oxide (MgO) thin film is the most suitable material for a protective layer in AC-PDP because of compatibility of anti-sputtering and secondary electron emission.[1)]

For industrial manufacturing, they have been extensively prepared by electron beam evaporation (EB) method with O_2 gas introduction and substrate heating. We have proposed the alternative MgO deposition using an advanced ion-plating (AIP) method[2)] and deposited MgO thin films for the protective layer for AC-PDPs.[3,4)]

In this paper, we measured the SEE from MgO thin films prepared by AIP and EB methods. The relation between SEE and film morphologies was discussed.

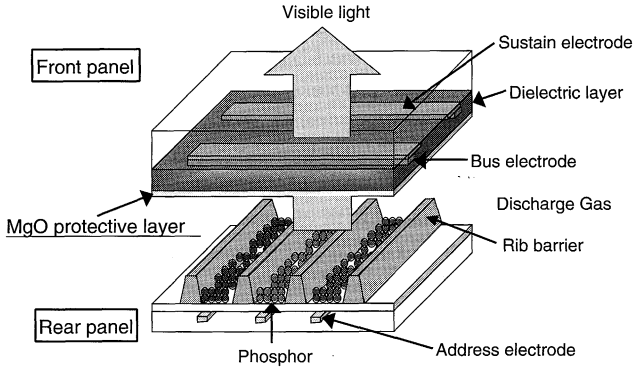

Fig. 1 Schematic diagram of typical AC-plasma display panel (AC-PDP).

2. Experimental

We deposited MgO thin films using the AIP method that we developed.[5)] A schematic diagram of the AIP apparatus is shown in Fig. 2. RF (13.56 MHz) and/or DC bias voltages are applied directly to the substrate holder. Plasma formed between the substrate holder and the chamber is regarded as a capacitor. Since the capacitance between the substrate holder and the chamber is small compared with the matching capacitance, it becomes easy to sustain plasma at lower pressures than other RF excitation ion-plating methods (above 10^{-3} Pa).[5)]

MgO thin films were deposited on silica glass plates and on stainless steel plates. Film thickness was 100 and 600 nm. RF power was 500 W and additional DC bias voltage was

*This Paper was Presented at the Autumn Meeting of the Japan Institute of Metals, held in Narashino, on March 30, 2001.

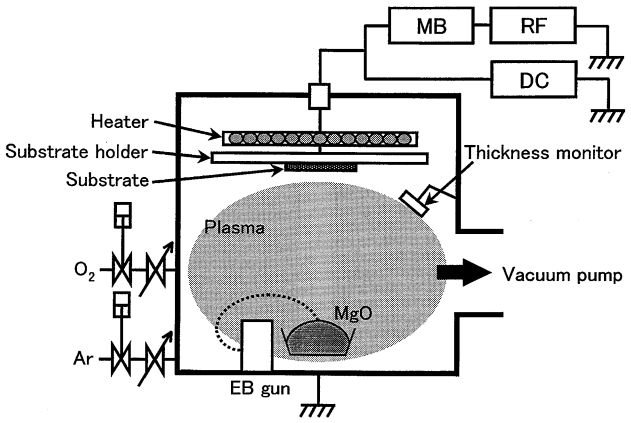

Fig. 2 Schematic diagram of the advanced ion-plating (AIP) apparatus. RF oscillator, matching box and DC power supply are denoted by RF, MB and DC, respectively.

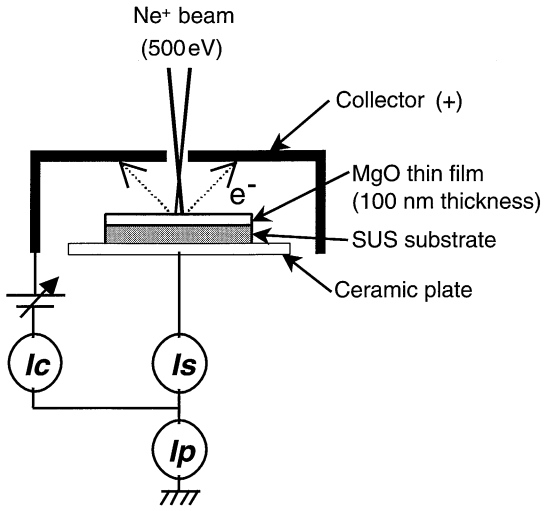

Fig. 3 Schematic diagram of setup for secondary electron measurement.

0–400 V. The substrate temperature was 473 K. Deposition rate was 1 nm/s. The base pressure of the chamber was below 6.7×10^{-4} Pa. Total gas pressure of Ar and O_2 gas mixture was 2×10^{-2} Pa. The target material was smashed single crystal MgO (purity: 99.9%). It was evaporated by an electron beam irradiation with beam scanning. Film thickness was determined by a quarts crystal monitor. We also deposited MgO thin films using a conventional electron beam evaporation (EB) method with the AIP apparatus (RF power was not applied). Deposition conditions in EB were same as these in AIP but with RF power.

We measured the secondary electron emission (SEE) of the films using the experimental setup shown in Fig. 3. Before the measurement, we irradiated the film with a Ne^+ beam to clean the surface. Beam current and acceleration voltage were 100 μA and 800 kV, respectively. We confirmed that the SEE current became stabilized by Ne^+ irradiation for 15 hours. The secondary electron yield, γ, is obtained from eq. (1), where I_c is the collector current and I_s is the specimen current.

$$\gamma = I_c/(I_s - I_c) \quad (1)$$

The γ was measured while increasing the collector bias voltage. The acceleration voltage of Ne^+ was 500 eV.

The crystal orientation of the MgO films was measured by x-ray diffraction (XRD) with $\theta/2\theta$ scanning. The x-ray used was monochromated $CuK_{\alpha 1}$ excitation ($\lambda = 0.15405$ nm). We observed the surface morphology and film texture by atomic force microscopy (AFM) and scanning electron microscopy (SEM), respectively.

3. Results and Discussion

We measured the SEE coefficient, γ, of MgO thin films deposited by AIP and EB methods. Figure 4 shows the γ as a function of the collector bias voltage, V_c, for AIP and EB films. The γ value sharply increased by increasing V_c and then became almost independent on V_c. Because MgO is an insulator, emitted electrons were forced back to the substrate due to the charging effects of the insulator. If the force by the collector bias voltage became larger than the back-force, all

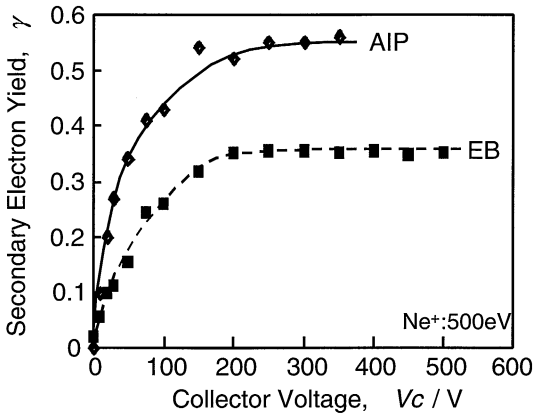

Fig. 4 The secondary electron emission coefficient, γ, as a function of the collector voltage, Vc, for the AIP and EB films. The γ for AIP was 0.55 and that for EB was 0.35.

of the emitted electrons could reach the collector electrode, as observed as a saturated γ in Fig. 4. The saturated γ is the definition of γ of the sample. In our measurements, the γ for the AIP film was thus obtained as 0.55, and as 0.35 for the EB film. The γ of EB film in this study is very close to the reported value by Choi *et al.*[6]

Figures 5(a) and (b) show the XRD patterns of AIP and EB films with a thickness of 100 nm deposited on glass substrates. They were prepared with the same procedure as for SEE samples. Figure 6 is the standard XRD pattern for MgO polycrystalline powder.[7] It is obvious that the AIP film was polycrystalline with (111) preferred orientation. On the other hand, the EB film had poor crystallinity with no preferred orientations. It is therefore suggested that crystal growth is rather promoted in AIP deposition compared with EB deposition.

Figures 7(a) and (b) shows the SEM images of the AIP and EB films with 100 nm thickness, respectively. The films were deposited on a silica glass plate in the same manner as SEE and XRD samples. The AIP film (Fig. 7(a)) consisted of well-defined columnar structures that reached from substrate interface to surface. It should be noted that every columnar

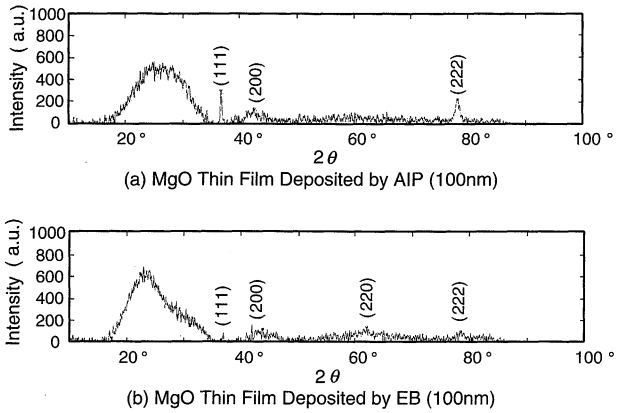

Fig. 5 XRD pattern of MgO thin film deposited by (a) AIP and (b) EB.

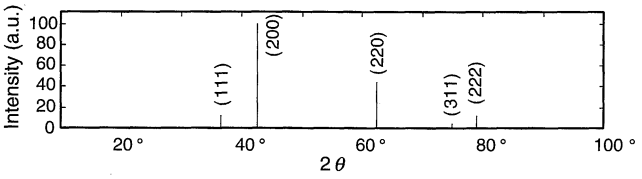

Fig. 6 XRD pattern for MgO polycrystalline powder.

structure ended up with a sharp apex and clear facets. They are probably {100} and/or {110} facets, which is now under investigation. The EB film had poor columns and the surface was rather flat and smooth than the AIP film (Fig. 7(b)), indicating that crystal growth was not promoted much.

We observed the surface morphologies using atomic force microscopy (AFM). Figures 8(a) and (b) shows AFM images of AIP and EB films with 100 nm thickness, respectively. In Fig. 8(a), crystal grains were uniformly observed on the surface; the number density of these grains was about 500 μm^{-2}. The EB film had a rather smooth surface with fine crystal grains (Fig. 8(b)). In Fig. 8(c), crystal grains became larger for the AIP film with a thickness of 600 nm. The number density of grains was about 400 μm^{-2}. It is supposed that the

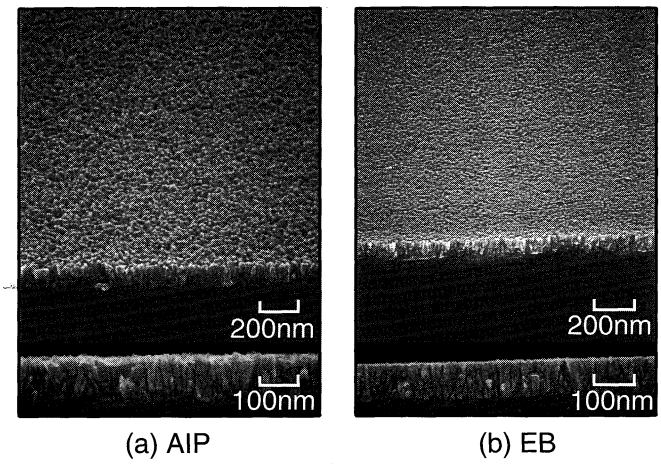

Fig. 7 SEM images of MgO thin films with 100 nm thickness deposited by (a) AIP and (b) EB.

columns emerged as the film growth proceeded.

For the growth of MgO films, atomic oxygen should react with Mg atoms. In EB deposition, oxygen molecules dissociate only by the substrate thermal energy, except for chemical reactions with the film surface. Whereas the AIP method, they dissociate not only by the thermal energy but also by the plasma excitation. Some of them are excited to higher energy states. Thus, oxidation reaction is further promoted by reactive oxygen in AIP deposition. In our previous papers,[3,4] we discussed that crystal growth in AIP was considerably promoted due to the efficient excitation of evaporated MgO in the plasma region. The AIP method features plasma operation at a lower pressure (10^{-2} Pa). Under such low pressures, mean free path is long and deactivation frequency is small. Thus, the energy loss of excited species would be small in the plasma region, resulting in excellent film growth.[5] Eventually, the excited species arrive at growth front without deactivation. We emphasize that with well-identified columnar structures that reached the surface from the substrate interface, sharp apex with facets and dense crystal grains were realized as a result of enhanced surface migration in the AIP deposition process.

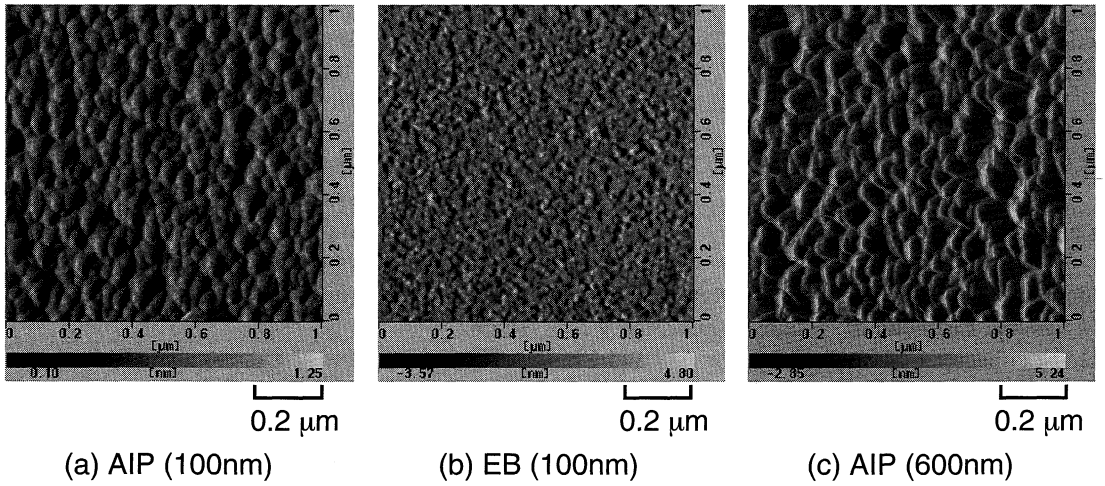

Fig. 8 AFM images of various MgO thin films.

Finally, we discuss the reason why the γ value was improved in AIP films. The (111) preferred orientation was reported to be suitable for secondary electron emission.[8] We have reported that EB films with 100 nm thickness had poor columnar structures and poor crystallinity: The AIP films with 100 nm thickness, on the other hand, had well-identified columnar structures and improved crystallinity with (111) preferred orientation. For an efficient SEE, electrons have to be continuously supplied from MgO crystals to vacuum. Thus, electron transport in MgO crystal is a key for SEE. It is well understood that electron transport is affected by defects in crystals regardless of carrier density. High quality MgO thin film is thus deeply desired for a high γ value. We emphasize that crystallinity of the MgO film was considerably improved by AIP depositions as already presented.[3,4] We suppose that the γ value was greatly improved due to the improved crystallinity as well as (111) preferred orientation.

4. Conclusion

We deposited MgO thin films as a protective layer in AC-PDPs using an advanced ion-plating (AIP) method and the conventional electron beam evaporation (EB) method. Then, we measured the secondary electron emissions from MgO thin films of 100 nm thickness using Ne^+ beam irradiation. The secondary electron yield, γ, of the AIP film is superior to that of the EB film. We supposed that it was due to the improved crystallinity as well as (111) preferred orientation.

Acknowledgements

The authors thank Prof. H. Uchiike of Saga University for fruitful advice on secondary electron measurements. We also appreciate Dr. Y. Tomioka of Hitachi Research Laboratory, Hitachi, Ltd. for his helpful discussions on AFM analysis.

REFERENCES

1) H. Uchiike, K. Miura, N. Nakayama, T. Shinoda and Y. Fukuyama: IEEE Trans. Electron Devices **ED-23** (1976) 1211–1217.
2) Japanese patent, No. 1560327.
3) K. Uetani, H. Kajiyama, A. Kato, A. Takagi, I. Tokomoto, Y. Koizumi, K. Nose, Y. Ihara, K. Onisawa and T. Minemura: Mater. Trans. **42** (2001) 411–413.
4) K. Uetani, H. Kajiyama, A. Kato, I. Tokomoto, Y. Koizumi, K. Nose, Y. Ihara, K. Onisawa and T. Minemura: Mat. Res. Soc. Symp. Proc. **647** (2001) O11.33.1-O11.33.6.
5) K. Uetani, H. Kajiyama, T. Yamaguchi, K. Nose, K. Onisawa and T. Minemura: Mater. Trans., JIM **41** (2000) 1161–1163.
6) E.-H. Choi, H.-J. Oh, Y.-G. Kim, J.-J. Ko, J.-Y. Lim, J.-G. Kim, D.-I. Kim, G. Cho and S.-O. Kang: Jpn. J. Appl. Phys. **37** (1998) 7015–7018.
7) JCPDS-card 75–0447 (1997).
8) H. Lin, Y. Harano and H. Uchiike: Tech. Rep. IEICE Jpn. EID95-51 (1995) 69–73.